Skeletal Muscle Triacylglycerol Hydrolysis Does Not Influence Metabolic Complications of Obesity

Mitch T. Sitnick,[1] Mahesh K. Basantani,[1] Lingzhi Cai,[1] Gabriele Schoiswohl,[1] Cynthia F. Yazbeck,[1] Giovanna Distefano,[1] Vladimir Ritov,[1] James P. DeLany,[1] Renate Schreiber,[2] Donna B. Stolz,[3] Noah P. Gardner,[4] Petra C. Kienesberger,[5] Thomas Pulinilkunnil,[5] Rudolf Zechner,[3] Bret H. Goodpaster,[1] Paul Coen,[1,6] and Erin E. Kershaw[1]

Intramyocellular triacylglycerol (IMTG) accumulation is highly associated with insulin resistance and metabolic complications of obesity (lipotoxicity), whereas comparable IMTG accumulation in endurance-trained athletes is associated with insulin sensitivity (the athlete's paradox). Despite these findings, it remains unclear whether changes in IMTG accumulation and metabolism per se influence muscle-specific and systemic metabolic homeostasis and insulin responsiveness. By mediating the rate-limiting step in triacylglycerol hydrolysis, adipose triglyceride lipase (ATGL) has been proposed to influence the storage/production of deleterious as well as essential lipid metabolites. However, the physiological relevance of ATGL-mediated triacylglycerol hydrolysis in skeletal muscle remains unknown. To determine the contribution of IMTG hydrolysis to tissue-specific and systemic metabolic phenotypes in the context of obesity, we generated mice with targeted deletion or transgenic overexpression of ATGL exclusively in skeletal muscle. Despite dramatic changes in IMTG content on both chow and high-fat diets, modulation of ATGL-mediated IMTG hydrolysis did not significantly influence systemic energy, lipid, or glucose homeostasis, nor did it influence insulin responsiveness or mitochondrial function. These data argue against a role for altered IMTG accumulation and lipolysis in muscle insulin resistance and metabolic complications of obesity. ***Diabetes*** **62:3350–3361, 2013**

Obesity is a global public health problem and a major risk factor for insulin resistance and type 2 diabetes. These disorders are characterized by excess lipid accumulation in multiple tissues, primarily as triacylglycerols (TAGs). The lipotoxicity hypothesis suggests that this lipid excess promotes cellular dysfunction and cell death, which ultimately contribute to insulin resistance and metabolic disease (1). However, intracellular TAG accumulation is not always associated with adverse metabolic outcomes, suggesting that TAGs themselves are not pathogenic (2). In contrast, other non-TAG lipid metabolites such as fatty acids (FAs), diacylglycerols (DAGs), and ceramides have been shown to influence glucose homeostasis and insulin action by interfering with insulin signaling and glucose transport, promoting endoplasmic reticulum stress and mitochondrial dysfunction, and activating inflammatory and apoptotic pathways (reviewed in ref. 3). Nevertheless, the precise identities and sources of these bioactive lipid intermediates remain elusive (4,5). Furthermore, whether intracellular TAGs serve as a protective sink or a toxic source of deleterious lipid metabolites that contribute to insulin resistance remains unclear (6).

Since skeletal muscle is the major contributor to insulin-mediated glucose disposal, lipid excess in this tissue could have serious implications for systemic glucose homeostasis and insulin responsiveness (7). Indeed, numerous studies have demonstrated a strong association between intramyocellular triacylglycerol (IMTG) accumulation and insulin resistance (reviewed in ref. 8). In contrast, endurance exercise training is characterized by IMTG accumulation and insulin sensitivity (the athlete's paradox) (2). This variable association between IMTG accumulation and insulin responsiveness has largely been attributed to differences in the balance between lipid delivery and muscle oxidative capacity (8–10). Not surprisingly then, most studies have focused on the impact of muscle FA uptake and/or oxidation on glucose homeostasis and insulin action (11). However, experimental manipulations of these parameters cannot distinguish among the effects of IMTGs, IMTG metabolism, and other lipid intermediates. Furthermore, accumulating evidence suggests that muscle oxidative capacity cannot entirely explain differences in IMTGs or insulin responsiveness (12). These findings have led to speculation that dynamic IMTG metabolism (i.e., TAG synthesis or hydrolysis) may be critically involved in lipid-induced insulin resistance (6). However, few studies have specifically addressed the contribution of IMTG metabolism per se to this process.

The regulated storage and release of IMTGs remain poorly understood, but require the coordinated action of synthetic enzymes (i.e., diacylglycerol acyltransferases [DGATs]), hydrolytic enzymes (i.e., adipose triglyceride lipase [ATGL] and hormone sensitive lipase [HSL]), and other lipid droplet proteins (6). Specifically, modulating IMTG synthesis in murine skeletal muscle alters IMTG content and systemic glucose homeostasis, supporting a role for IMTG metabolism in metabolic disease (13–15). However, the metabolic impact of modulating IMTG hydrolysis in vivo remains unclear. Global deletion of either ATGL (16–19) or HSL (20) has produced variable results.

From the [1]Division of Endocrinology, Department of Medicine, University of Pittsburgh, Pittsburgh, Pennsylvania; the [2]Institute of Molecular Biosciences, University of Graz, Graz, Austria; the [3]Department of Cell Biology, University of Pittsburgh, Pittsburgh, Pennsylvania; the [4]Novartis Institute of Biomedical Research, Cambridge, Massachusetts; the [5]Department of Biochemistry and Molecular Biology, Dalhousie University, Dalhousie Medicine New Brunswick, Saint John, New Brunswick, Canada; and the [6]Department of Health and Physical Activity, University of Pittsburgh, Pittsburgh, Pennsylvania.

Received 4 April 2013 and accepted 10 June 2013.
DOI: 10.2337/db13-0500
This article contains Supplementary Data online at http://diabetes.diabetesjournals.org/lookup/suppl/doi:10.2337/db13-0500/-/DC1.

Corresponding author: Erin E. Kershaw, kershawe@pitt.edu.

M.T.S., M.K.B., and L.C. contributed equally to this work.

The former, but not the latter, results in massive IMTG accumulation with improvement in systemic glucose homeostasis, suggesting that inhibition of ATGL-mediated TAG hydrolysis protects against insulin resistance. In contrast, recent studies in cardiac muscle (21) and other tissues (22,23) indicate that ATGL-mediated TAG hydrolysis is required for mitochondrial function such that enhancing, rather than inhibiting, ATGL action may improve metabolic outcomes. Nevertheless, the autonomous role of skeletal muscle TAG catabolism in influencing muscle-specific and systemic metabolic phenotypes remains unknown.

The goal of the current study was to understand the contribution of IMTG hydrolysis to tissue-specific and systemic metabolic phenotypes, particularly glucose homeostasis and insulin action, in the context of obesity. We therefore generated animal models with decreased (skeletal muscle-specific ATGL knockout [SMAKO] mice) and increased (muscle creatine kinase [Ckm]-ATGL transgenic [Tg] mice) ATGL action exclusively in skeletal muscle, and assessed the metabolic consequences at baseline and in response to chronic high-fat feeding. Interestingly, modulation of IMTG hydrolysis via ATGL action did not significantly influence glucose homeostasis, insulin action, or other metabolic phenotypes in the context of obesity despite dramatic changes in IMTG content.

RESEARCH DESIGN AND METHODS

Animals. SMAKO mice were generated by crossing B6.129-Pnpla2^{tm1Eek} (ATGL-flox) mice with Myo-Cre mice (24). Ckm-ATGL Tg mice were generated by cloning murine ATGL in front of the Ckm promoter (25). B6.129-Pnpla2^{tm1Eek}, SMAKO, and Ckm-ATGL mice were generated as described in Figs. 2*A* and 5*A* and the Supplementary Data online. Male ATGL$^{flox/flox}$ Cre/+ mice were mated to female ATGL$^{flox/flox}$+/+ mice to generate ATGL$^{flox/flox}$ Cre/+ (SMAKO) and ATGL$^{flox/flox}$ +/+ (control) mice. Male Ckm-ATGL Tg mice were mated to female wild-type (WT) mice to generate Tg and WT mice. Global ATGL knockout (ATGL$^{-/-}$ or GAKO) mice have been previously reported (16,17). Mice were housed under standard conditions (25°C, 14:10-h light/dark cycle) with ad libitum access to chow (Prolab Isopro RMH 3000; 14 kcal% fat) or high-fat diet (HFD; Research Diets D12451i, 45 kcal% fat). Body composition, energy expenditure, and metabolic parameters were performed as described (26). Experiments were approved by the University of Pittsburgh Institutional Animal Care and Use Committee and conducted in conformity with the Public Health Service Policy for Care and Use of Laboratory Animals.

Lipid analyses. DAGs (27), ceramides (27), and long-chain FA-CoAs (28) as well as TAG hydrolase activities (26) and radiolabeled palmitate oxidation (29) were determined in muscle homogenates and normalized to tissue wet weight or protein content.

Mitochondrial respiration. Respirometry was performed in permeabilized myofiber bundles using an Oxygraph-2K (Oroboros) (30). Assays were run at 37°C in oxygen-saturated (~150–220 μmol O_2) buffer (105 mmol K-MES, 30 mmol KCl, 10 mmol KH_2PO_4, 5 mmol $MgCl_2$, 5 mg/mL BSA, and 1 mmol EGTA [pH 7.4]) containing 25 μmol blebbistatin using the following titration protocol: 20 μmol palmitoylcarnitine, 2 mmol malate, 4 mmol ADP, 5 mmol glutamate, 10 mmol succinate, 10 μmol cytochrome c, 10 μg/mL oligomycin, and 2 μmol carbonylcyanide-*p*-trifluoromethoxyphenylhydrazone. Respiration rates were normalized to myofiber dry weight.

Insulin signaling and protein expression. Insulin signaling studies were performed (17) using the following primary antibodies: anti-pAkt (pT308) (4056S; Cell Signaling Technology), anti-pAkt (pS473), and anti-Akt (total) (05-736 and 07-416; EMD Millipore). For protein expression under non–insulin-stimulated conditions, the following antibodies were used: MitoProfile Antibody Cocktail (MS604; Mitosciences), anti-HSL (4017s; Cell Signaling Technology), anti-pHSL (S565 and S660) (4137S and 4126S; Cell Signaling Technology), antiperilipint (Plin)2 (20R-AP002; Fitzgerald Industries), anti-Plin5 (03-GP31; American Research Products), anti-ATGL (2439; Cell Signaling Technology), and anti-CGI58 (NB110-41576; Novus Biologicals). For loading controls, the following antibodies were used: anti-Ran GTPase (610340; BD Biosciences) or β-actin (4970; Cell Signaling Technology). Visualization was performed with Immun-Star WesternC Chemiluminescent Kit in a VersaDoc System and quantified using Quantity One 1-D software (Bio-Rad).

Tissue imaging. Muscles were frozen in isopentane in OCT and cut into 10-μm sections. For muscle morphology, sections were stained with hematoxylin and eosin (H&E). Alternatively, sections were processed for neutral lipid content (using Oil Red O [ORO]) and/or expression of specific proteins (using ATGL or other antibodies noted above) either alone or in combination with fiber type–specific antibodies from the Developmental Studies Hybridoma Bank (A4.840 [1], A4.74 [2A], 6H1 [2X], 10F5 [2B]) followed by secondary antibodies (A21044 and A10035; Invitrogen) (31). At least four random areas were visualized (DM4000B; Leica Microsystems), digitally captured (Retiga-2000R; QImaging), and quantified (Northern Eclipse; Empix Imaging). For transmission electron microscopy (TEM), muscles were fixed in 2.5% glutaraldehyde, postfixed in 1% osmium tetroxide, dehydrated, embedded in epon, and evaluated by TEM (JEM-1011; JEOL).

Gene expression. RNA extraction, reverse transcription, and gene expression analysis were performed using an Eppendorf Realplex System in accordance with Minimum Information for Publication of Quantitative Real-Time PCR Experiments (MIQE) guidelines (17,26).

Statistical analysis. Results are expressed as mean ± SEM. Comparisons were made by unpaired two-tailed Student *t* test or factorial ANOVA followed by determination of simple effects for pairwise comparisons. If indicated, comparisons were made by two-way ANOVA with repeated measures. For energy expenditure data, comparisons were made using generalized estimate equations. *P* values of <0.05 were considered statistically significant.

RESULTS

Endogenous ATGL expression in murine skeletal muscle is fiber type–specific and regulated by HFD feeding. Fiber type–specific quantitative immunofluorescence (IF) revealed that endogenous ATGL was predominantly expressed in type 2A and 2X fibers with lower expression in type 1 fibers and minimal expression in type 2B fibers (Fig. 1*A* and *C* and Supplementary Fig. 1*A* and *B*). Conversely, global deletion of ATGL resulted in fiber type–specific accumulation of IMTGs in types 2A, 2X, and 1 fibers (Fig. 1*B* and Supplementary Fig. 1*C*). The distribution of these fibers differs among murine muscles (Supplementary Fig. 1*D*). Endogenous ATGL protein directly correlated with IMTG content (Fig. 1*E*) and also increased in parallel with IMTGs following HFD feeding (Fig. 1*C–E*). Thus, endogenous ATGL is expressed and functional in type 2A > 2X > 1 murine muscle fibers and increases with diet-induced obesity.

Reducing IMTG hydrolysis via ATGL deletion increases IMTG content and subspecies of DAGs, but does not significantly influence other intramyocellular lipids or systemic lipid homeostasis. To reduce IMTG hydrolysis, SMAKO mice were generated by crossing ATGL-flox mice with Myo-Cre mice (24) (Fig. 2*A*). SMAKO mice had reduced ATGL mRNA (Fig. 2*B*) and protein (Fig. 2*C*) in skeletal but not cardiac muscle or other tissues. Accordingly, TAG hydrolase activity in skeletal muscle of SMAKO mice was dramatically reduced, could not be stimulated with the ATGL coactivator CGI-58, and was completely blunted in the presence of an HSL inhibitor (Fig. 2*D*). General muscle morphology did not differ between genotypes (Fig. 2*E*, *top*). Fiber type–specific quantitative IF of IMTG content, which is more sensitive and specific than whole-muscle biochemical IMTG analysis, revealed a dramatic fiber type–specific (2A > 2X > 1, but not 2B) increase in IMTGs in skeletal muscle of SMAKO mice that was comparable to GAKO mice (Fig. 2*E* and *F*). Cardiac muscle, in contrast, was unaffected (Supplementary Fig. 2). Lipidomic analysis of skeletal muscle (Fig. 2*G*) revealed no significant genotype effect on total DAGs, ceramides, or FA-CoAs. However, there was a trend toward increased total DAGs similar to GAKO mice (17). A detailed analysis of lipid classes in skeletal muscle revealed an effect of genotype on a few subspecies of DAGs (C14:0/C16:0-DAG, C14:0/C18:0-DAG, and C16:0/C18:0-DAG) and FA-CoAs (C14:0 and C16:0) (Supplementary Fig. 3). Finally, serum

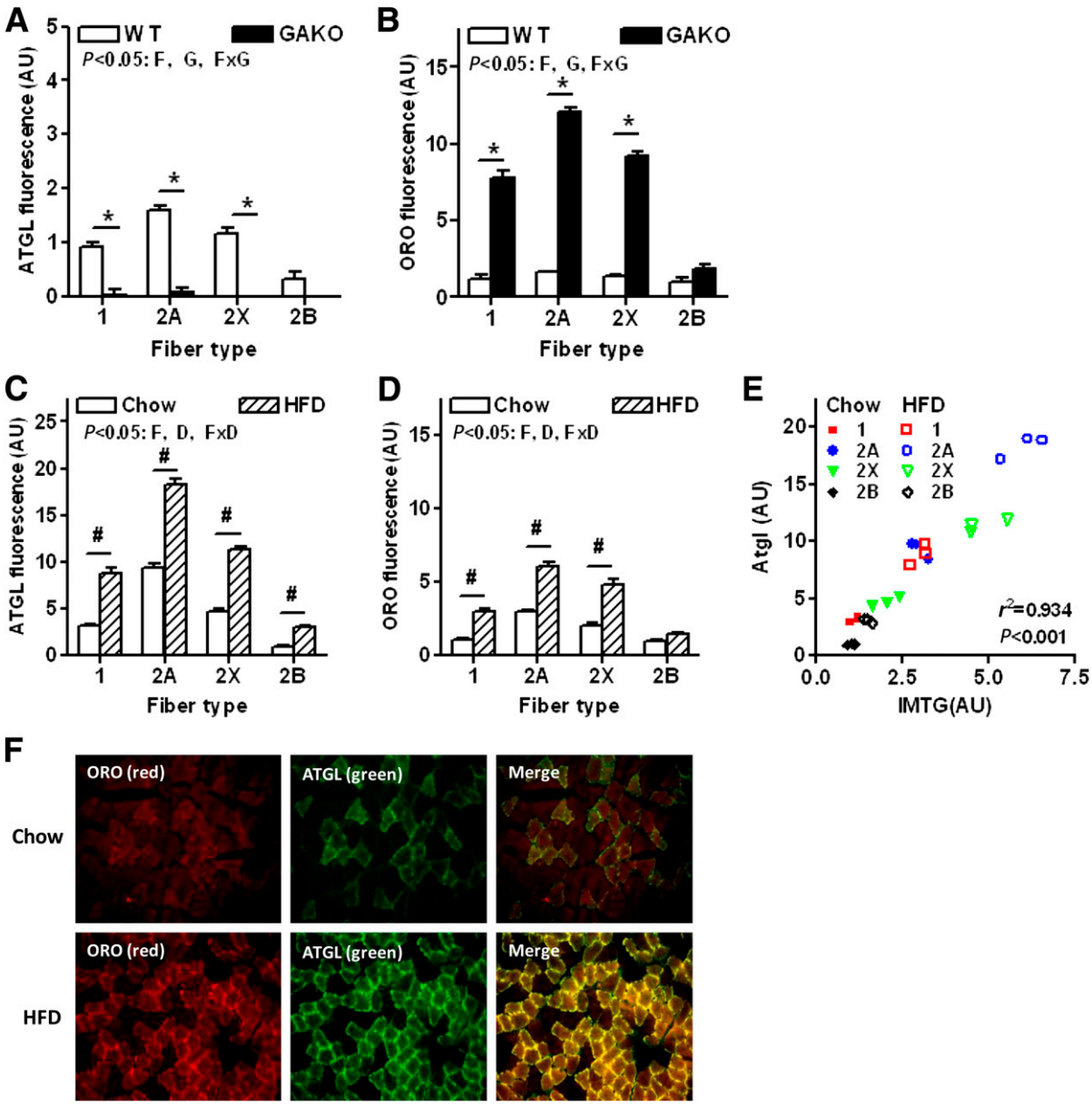

FIG. 1. Fiber type–specific expression of endogenous ATGL in murine skeletal muscle and regulation by HFD feeding. ATGL protein expression (ATGL IF in 2B fibers of GAKO mice set to 0) (*A*) and IMTG content by ORO staining (ORO IF of 2B fibers of WT mice set to 1) (*B*) in skeletal muscle fibers of chow-fed WT versus GAKO mice (♀, chow, 10 weeks, C57BL/6, gastrocnemius-plantaris-soleus [GPS] complex; *n* = 3 to 4/group). ATGL protein expression (ATGL IF in 2B fibers of WT-chow mice set to 1) (*C*) and IMTG content by ORO staining (ORO IF in 2B fibers of WT-chow mice set to 1) (*D*) in skeletal muscle fibers of chow- versus HFD-fed WT mice (♀, 22 weeks FVB, GPS complex; *n* = 3 to 4/group). *E*: Relationship between ATGL and IMTG (data from *C* and *D*). *F*: Representative images of ATGL and ORO IF in chow- and HFD-fed mice demonstrating overlap and enhanced staining with HFD. For overall effects having $P < 0.05$: D, diet; F, fiber type; G, genotype. For specific comparisons having $P < 0.05$: #for effect of diet; *for effect of genotype. AU, arbitrary units.

TAGs (Control-HFD 60 ± 5 vs. SMAKO-HFD 62 ± 5 mg/dL) and nonesterified FAs (Control-HFD 0.59 ± 0.05 vs. SMAKO-HFD 0.65 ± 0.06 mEq/L) did not differ between genotypes. Thus, decreasing IMTG hydrolysis via ATGL increases certain subspecies of DAGs and tends to increase total DAGs, but does not produce significant changes in other non-TAG intramyocellular lipids or systemic lipid homeostasis despite dramatic increases in IMTG content.

Reducing IMTG hydrolysis via ATGL deletion increases lipid droplet proteins but does not influence mitochondrial phenotypes. Skeletal muscle FA oxidation increased with HFD feeding but was unaffected by genotype (Fig. 3*A*). Likewise, mitochondrial respiration in isolated muscle fibers failed to identify any genotype effects in basal, substrate-stimulated, or uncoupled conditions (Fig. 3*B*). Consistent with these results, expression of mitochondrial oxidative phosphorylation proteins was not different between genotypes (Fig. 3*C*). Furthermore, imaging by TEM (Fig. 3*D*) and confocal microscopy (Supplementary Fig. 4) revealed no differences between genotypes for mitochondrial morphology or number, despite massive increases in lipid droplet size and number. Gene expression analysis revealed an increase in peroxisome proliferator–activated receptor (PPAR) α expression in chow- but not HFD-fed SMAKO mice (although threshold cycle was >35 using undiluted cDNA), but no effect of genotype on PPARδ, PPARγ

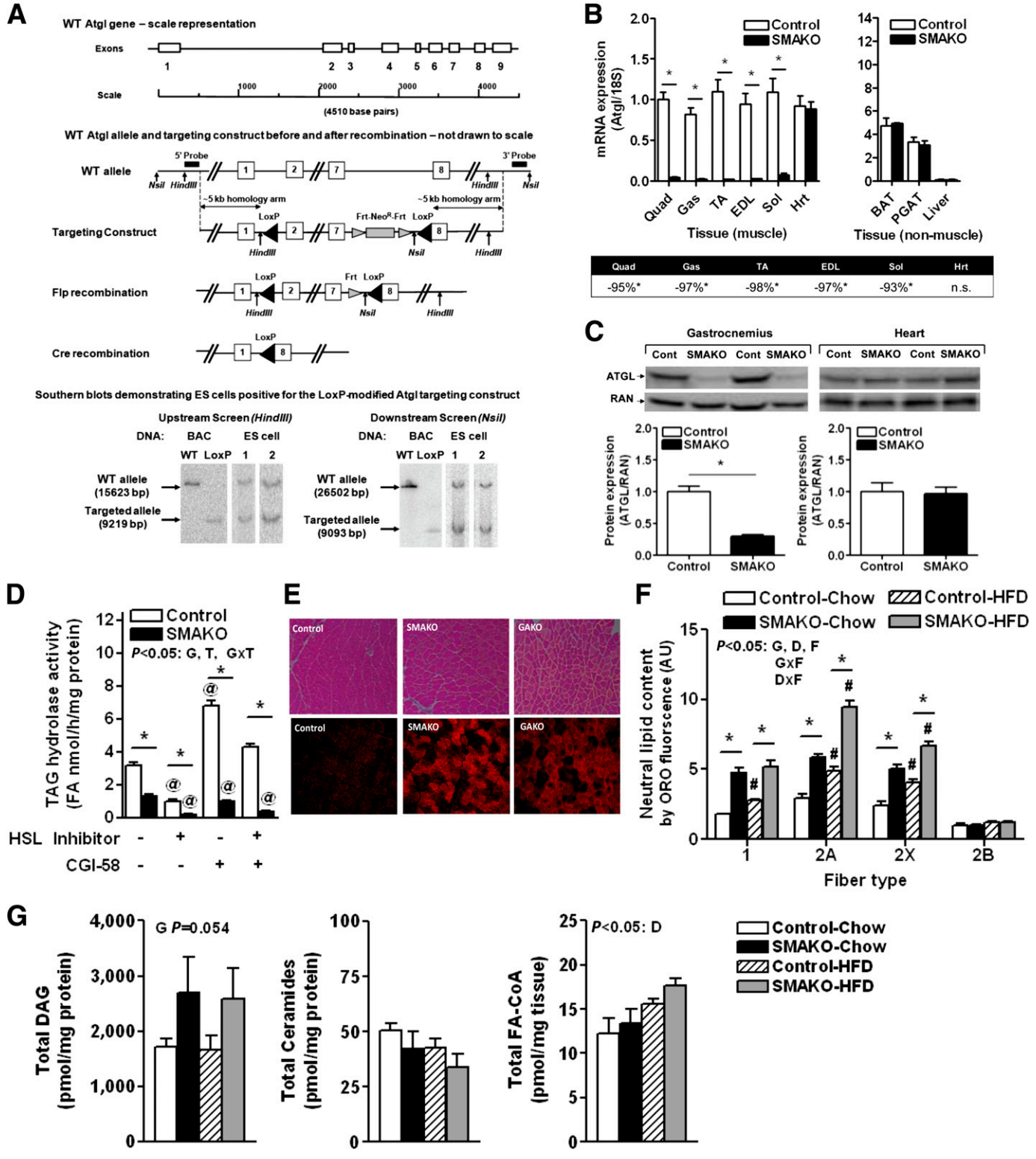

FIG. 2. Skeletal muscle–specific ATGL deletion and its impact on lipid homeostasis in SMAKO mice. *A*: The LoxP-modified ATGL construct. *B*: ATGL mRNA expression relative to 18S control gene by quantitative PCR in muscle and nonmuscle tissues with endogenous ATGL expression in quadriceps arbitrarily set to 1 (♀, 10 weeks, chow, fasted 12 h; $n = 5$ to 6/group). Percent decrease in ATGL mRNA expression in SMAKO relative to WT mice for select muscle tissues is shown in the table (*bottom*). *C*: ATGL protein expression relative to Ran GTPase (RAN) control in skeletal versus cardiac muscle (♀, 10 weeks, chow, fasted 12 h, gastrocnemius and heart; $n = 5$ to 6/group). *D*: TAG hydrolase activity at baseline and in the presence of the HSL-specific inhibitor 76-0079, the ATGL-specific activator CGI-58, or HSL inhibitor plus CGI-58 (♂, 28 weeks, chow, fasted 12 h, red gastrocnemius; $n = 6$/group). *E*: Skeletal muscle histology of control (*left*), SMAKO (*middle*), and GAKO (*right*) mice including general morphology by H&E staining (*top*) and IMTG content by ORO staining (*bottom*) (♂, 28 weeks, chow, fasted 12 h, gastrocnemius-plantaris-soleus [GPS] complex). *F*: IMTG content by ORO staining using quantitative IF (♂, 28 weeks, fasted 12 h, GPS complex, average of four muscle areas each; $n = 4$/group). Type 2B fibers of chow-fed WT mice are arbitrarily set to 1. *G*: Intramyocellular DAG, ceramide, and FA-CoA content using biochemical analysis of whole muscle (♂, 28 weeks, fasted 12 h, quadriceps; $n = 3$ to 4/group). For overall effects having $P < 0.05$: D, diet; F, fiber type; G, genotype; T, treatment (with HSL-inhibitor or CGI-58). For specific comparisons having $P < 0.05$: #for effect of diet; *for effect of genotype; and @for effect of treatment. AU, arbitrary units; BAC, bacterial artificial chromosome; BAT, brown adipose tissue; D, diet; EDL, extensor digitorum longus; ES, embryonic stem; Gas, gastrocnemius; Hrt, heart; PGAT, perigonadal adipose tissue; Quad, quadriceps; Sol, soleus; TA, tibialis anterior.

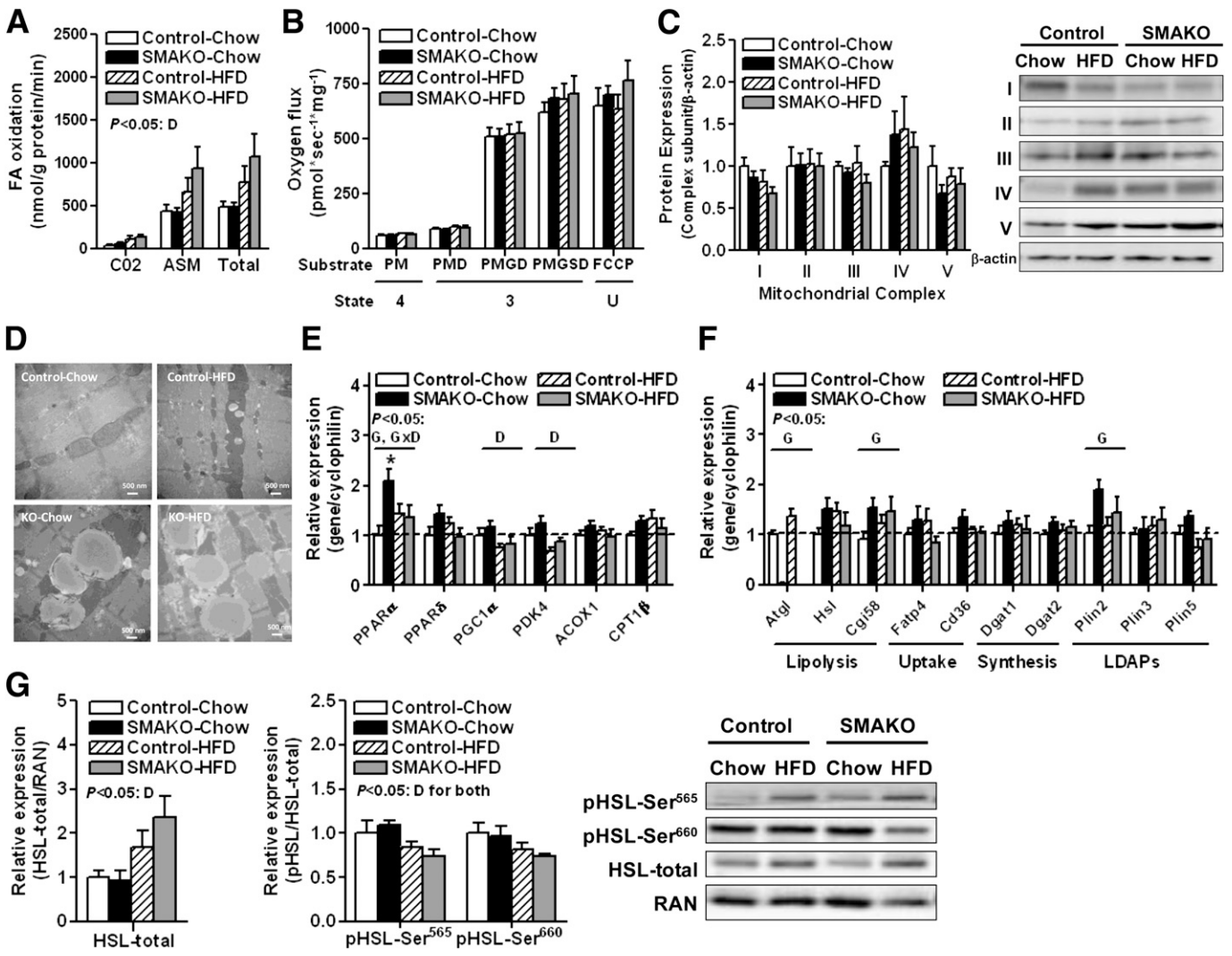

FIG. 3. Skeletal muscle mitochondrial function and expression of genes/proteins regulating lipid homeostasis in SMAKO mice. *A*: FA oxidation (♂, 28 weeks, fasted 12 h, red gastrocnemius; n = 6/group). ^{14}C-labeled incorporation into CO_2 and acid-soluble metabolites (ASMs) represent complete and incomplete oxidation, respectively. *B*: Mitochondrial respiration in permeabilized muscle fibers (♂, 28 weeks, fasted 12 h, soleus; n = 6/group). Oxygen consumption was measured following the sequential addition of the following substrates: palmitoylcarnitine (P), malate (M), ADP (D), glutamate (G), succinate (S), and cytochrome c, oligomycin, and carbonylcyanide-*p*-trifluoromethoxyphenylhydrazone (FCCP). The corresponding respiratory states are noted: ADP-driven respiration (state 3), respiration in the absence of ADP (state 4), and uncoupled respiration (state U). *C*: Expression of oxidative phosphorylation proteins in complexes I–V (NDUFB8 [complex I], SDHB [complex II], UQCRC2 [complex III], MTCO1 [complex IV], and ATP5A [complex V]) (♂, 28 weeks, fasted 12 h, tibialis anterior; n = 6/group). Data are normalized to protein expression of β-actin. *D*: TEM of skeletal muscle (♂, 28 weeks, fasted 12 h, red quadriceps, representative images). mRNA expression of PPARα/PGC1α and their target genes (*E*) and genes for lipid breakdown (lipolysis), uptake, and synthesis as well as lipid droplet–associated proteins (LDAPs) of the Plin family (*F*) relative to cyclophilin control with expression in WT-chow normalized to 1 (♂, 28 weeks, tibialis anterior; n = 9–13/group). *G*: Protein expression of total HSL normalized to Ran GTPase (RAN) control (*left*), phosphorylated HSL normalized to total HSL (*middle*), and representative immunoblots (*right*) (♂, 28 weeks, tibialis anterior; n = 4/group). For mRNA and protein expression, samples were confirmed to have low or no expression of Plin1, thereby confirming absence of significant fat contamination. For overall effects having $P < 0.05$: D, diet; G, genotype. Where an interaction was identified, specific comparisons having $P < 0.05$: *for effect of genotype.

coactivator (PGC) 1α, or PPAR target genes (Fig. 3*E*). ATGL mRNA expression was clearly decreased (>90%) in SMAKO muscle (Fig. 3*F*). However, expression of total HSL mRNA (Fig. 3*F*) and protein (Fig. 3*G*) as well as phosphorylation of HSL at Ser565 (AMPK target site, negative regulator of HSL action) and Ser660 (ERK target site, positive regulator of HSL action) (Fig. 3*G*) were unchanged. Likewise, no effects of genotype were identified on mRNA expression for genes involved in lipid uptake (FATP1 and CD36) or synthesis (DGAT1 and DGAT2). In contrast, CGI-58 and Plin2/Adrp mRNA (Fig. 3*F*) as well as CGI-58, Plin2/Adrp, and Plin5/Oxpat protein (Supplementary Fig. 5) were increased in SMAKO mice. However, these mechanisms were clearly inadequate to compensate for loss of ATGL. Thus, reduced TAG hydrolysis in skeletal muscle does not influence lipid oxidation or mitochondrial phenotypes.

Reducing IMTG hydrolysis via ATGL deletion does not influence systemic energy homeostasis, glucose homeostasis, or insulin action. As expected, HFD feeding increased adiposity (Fig. 4*A* and *B*), altered energy substrate utilization (Fig. 4*E*), and impaired both glucose tolerance (Fig. 4*F*) and insulin sensitivity (Fig. 4*G–K*). In contrast, there were no effects of genotype on body weight (Fig. 4*A*), fat mass (Fig. 4*B*), lean mass (Fig. 4*C*), individual muscle weights (Fig. 4*D*), nonmuscle tissue weights (data not shown), or total energy intake and expenditure (data

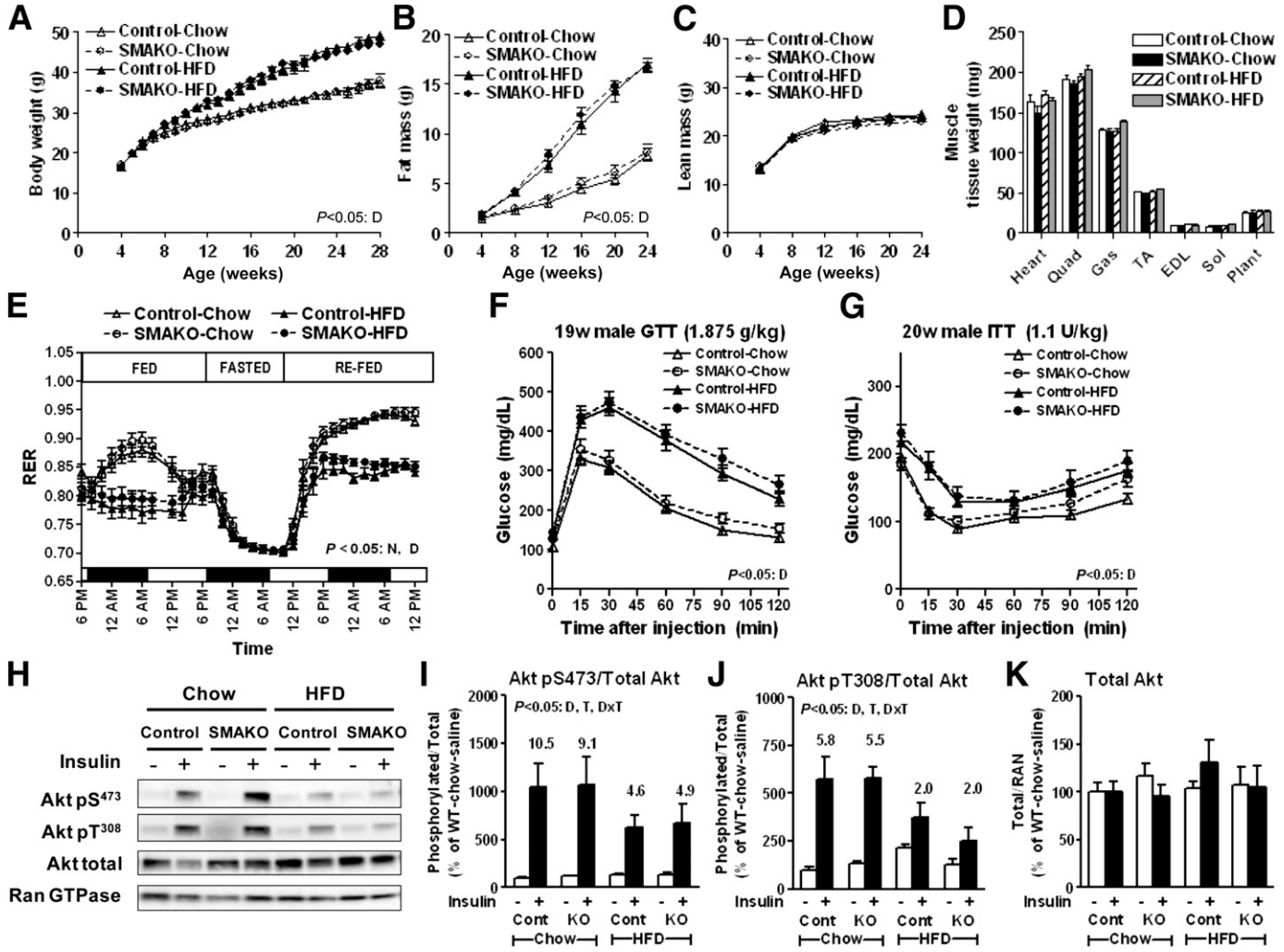

FIG. 4. Energy/glucose homeostasis and insulin action in SMAKO mice. Body weight (*A*), fat mass (*B*), and lean mass (*C*) (♂, 3–28 weeks; $n \geq 19$/group). *D*: Muscle weights. With the exception of heart, data represent the average weight for both muscles from each mouse (♂, 28 weeks, fasted 12 h; $n \geq 19$/group). EDL, extensor digitorum longus; Gas, gastrocnemius; Hrt, heart; Plant, plantaris; Quad, quadriceps; Sol, soleus; TA, tibialis anterior. *E*: RER using a Comprehensive Lab Animal Monitoring System (CLAMS) (♂, 11 weeks, weight-matched; $n = 4$/group). *F*: GTT at 19 weeks with 1.875 g/kg glucose i.p. (♂, fasted 12 h; $n = 17$–20/group). *G*: ITT at 20 weeks with 1.1 units/kg insulin i.p. (♂, fasted 4 h; $n = 17$–20/group). *H–K*: Insulin signaling studies: mice were fasted for 12 h, injected i.p. with saline or insulin at 10 units/kg body weight, and killed 10 min thereafter (♂, 28 weeks, tibialis anterior; $n = 5$–7/group). Representative immunoblots (*H*) and associated quantification of stoichiometric phosphorylation of Akt pS^{473}/Akt total (*I*), Akt pT^{308}/Akt total (*J*), and total Akt/Ran GTPase (RAN) control (*K*). Fold change in response to insulin treatment is indicated above the black bars. For overall effects having $P < 0.05$: D, diet; G, genotype; N, nutritional status (i.e., fasting/refeeding); T, treatment (i.e., with insulin). For clarity, only overall effects are shown.

not shown). Although alterations in IMTG metabolism could influence metabolic flexibility without affecting overall energy homeostasis, energy utilization (respiratory exchange ratio) during ad lib feeding, fasting, and refeeding transitions was likewise unchanged between genotypes (Fig. 4*E*). In addition, no differences in serum glucose were identified between genotypes following a physiological (4-h) fast (Fig. 4*G*, time 0 of insulin tolerance test [ITT]), a prolonged (12-h) fast (Fig. 4*F*, time 0 of glucose tolerance test [GTT]), an intraperitoneal glucose challenge (Fig. 4*F*, GTT), or an intraperitoneal insulin challenge (Fig. 4*G*, ITT). Consistent with these findings, diet but not genotype effects were identified in skeletal muscle–specific insulin-stimulated phosphorylation of key proteins in the insulin signaling cascade including insulin receptor substrate 1 (data not shown) and Akt (Akt pS^{473} or Akt pT^{308}) (Fig. 4*H–K*). Thus, decreasing IMTG hydrolysis via ATGL deletion does not influence systemic energy homeostasis in the setting of acute or chronic nutritional challenges, nor does it influence systemic or muscle-specific glucose homeostasis and insulin action.

Increasing IMTG hydrolysis via ATGL overexpression decreases IMTG content but does not change other intramyocellular lipids or systemic lipid homeostasis. To increase IMTG hydrolysis, we generated skeletal muscle–specific Ckm-ATGL Tg mice (Fig. 5*A*). Tg founder lines had increased ATGL mRNA (Fig. 5*B*) and protein (Fig. 5*C*) in skeletal but not cardiac muscle or other tissues. Notably, skeletal muscle ATGL mRNA expression in Tg mice was comparable to endogenous ATGL expression in adipose tissue (32). IF analysis confirmed an increase in ATGL protein expression within all skeletal muscle fiber types of Tg mice (Fig. 5*D* and *E*). Thus, ATGL transgene expression overlaps with endogenous ATGL expression. Tg muscle TAG hydrolase activity also increased in an ATGL-specific manner since it was increased in the presence of an HSL inhibitor (Fig. 5*F*). General muscle morphology did not differ between

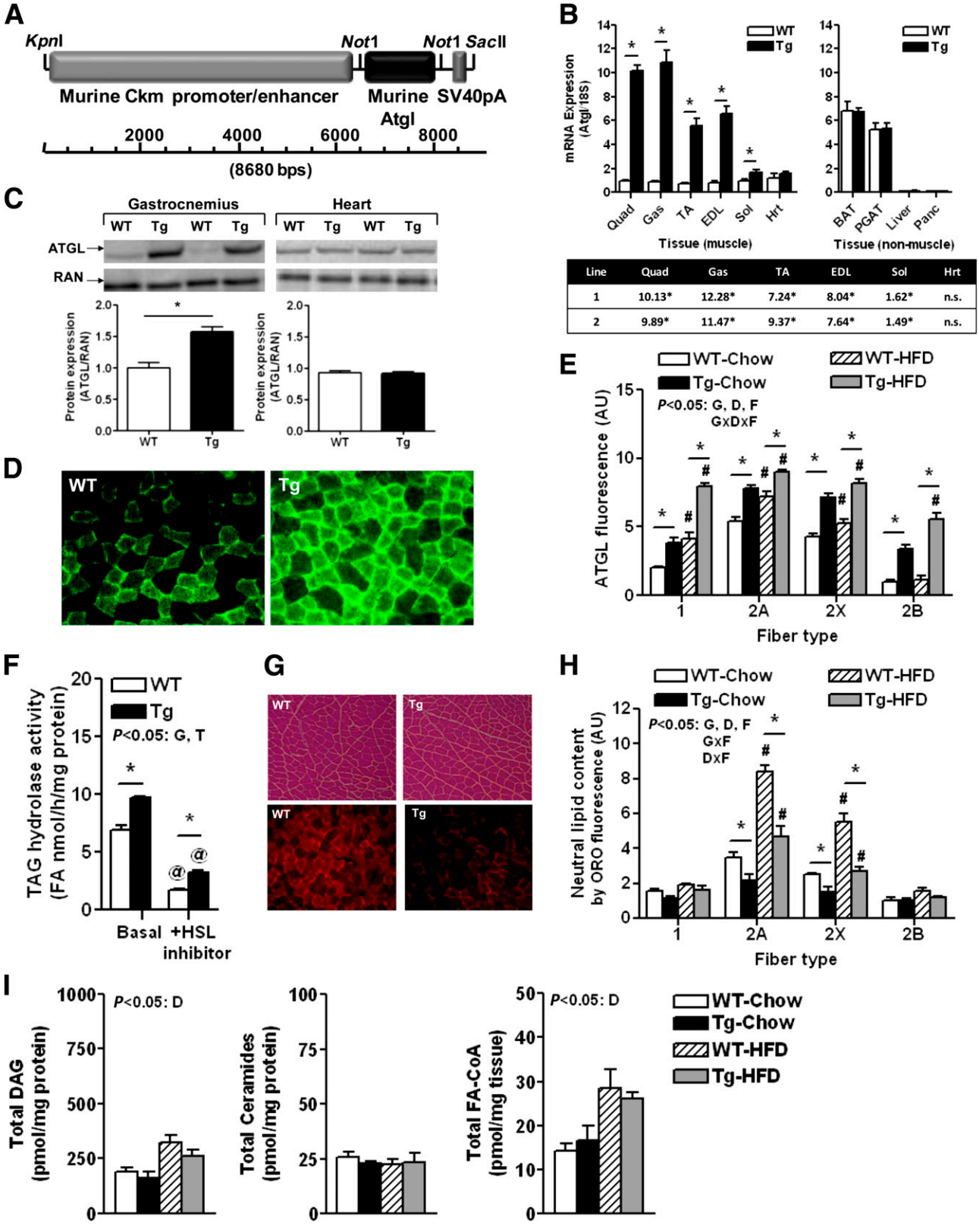

Line	Quad	Gas	TA	EDL	Sol	Hrt
1	10.13*	12.28*	7.24*	8.04*	1.62*	n.s.
2	9.89*	11.47*	9.37*	7.64*	1.49*	n.s.

FIG. 5. Skeletal muscle–specific overexpression of ATGL and its impact on lipid homeostasis. *A*: The Ckm-ATGL transgene construct. *B*: ATGL mRNA expression relative to 18S control gene by quantitative PCR in muscle and nonmuscle tissues with endogenous ATGL expression in quadriceps arbitrarily set to 1 (Line 1, ♀, 8 weeks, chow, fasted 12 h; *n* = 4–5/group). The fold-increase in ATGL mRNA expression in Tg relative to WT mice for select muscle tissues in each of two founder lines is shown in the table (*bottom*). *C*: ATGL protein expression relative to Ran GTPase (RAN) control as determined by immunoblotting in skeletal versus cardiac muscle (Line 1, ♀, 17 weeks, chow, fasted 12 h, gastrocnemius and heart; *n* = 6/group). *D*: ATGL IF in skeletal muscle (Line 1, ♂, 17 weeks, chow, fasted 12 h, gastrocnemius). *E*: Quantitative fiber type–specific ATGL protein expression by IF (Line 1, ♂, 28 weeks, chow and HFD, fasted 12 h, gastrocnemius-plantaris-soleus [GPS] complex, average of four muscle areas each; *n* = 4/group). Type 2B fibers of chow-fed WT mice are arbitrarily set to 1. *F*: TAG hydrolase activity in the absence (basal) and presence of the HSL-specific inhibitor 76-0079 (Line 1, ♂, 12 weeks, chow, fasted 12 h, gastrocnemius; *n* = 3/group). *G*: Skeletal muscle histology of

genotypes (Fig. 5*G*, *top*). However, IMTGs were dramatically decreased in Tg mice with the greatest reduction in type 2A and 2X fibers (Fig. 5*G* and *H*). Lipidomic analysis of skeletal muscle (Fig. 5*I*) revealed no genotype effects on total DAGs, ceramides, or FA-CoAs. Furthermore, there was an effect of diet but not genotype on multiple subspecies of DAGs, ceramides, and FA-CoAs, with the only exceptions being reduced C16:0 ceramide and sphingosine (Supplementary Fig. 6). Furthermore, serum concentrations of TAGs (WT-HFD 122 ± 12 vs. Tg-HFD 126 ± 12 mg/dL) and nonesterified FAs (WT-HFD 0.62 ± 0.05 vs. Tg-HFD 0.59 ± 0.07 mEq/L) did not differ between genotypes. Thus, increasing IMTG hydrolysis via ATGL overexpression does not produce major changes in non-TAG intramyocellular lipids or systemic lipid homeostasis despite dramatic reductions in IMTG content.

Increasing IMTG hydrolysis via ATGL overexpression does not influence other pathways of lipid metabolism or mitochondrial phenotypes. As with SMAKO mice, FA oxidation was increased by HFD feeding but was unaffected by genotype (Fig. 6*A*). Likewise, mitochondrial respiration in isolated muscle fibers (Fig. 6*B*) and expression of mitochondrial proteins (Fig. 6*C*) did not differ between genotypes. Furthermore, TEM revealed no differences between genotypes for mitochondrial morphology or number, despite a clear reduction in lipid droplet size and number (Fig. 6*D*). Gene expression analysis revealed diet but not genotype effects on PPARα, PPARδ, PGC1α, and their target genes (Fig. 6*E*). ATGL mRNA expression was clearly increased (>12-fold) in skeletal muscle of Tg mice (Fig. 6*F*). However, expression of total HSL mRNA (Fig. 6*F*) and protein (Fig. 6*G*) as well as phosphorylation of HSL at Ser565 and Ser660 (Fig. 6*G*) were unchanged in Tg mice. Likewise, expression of other genes involved in lipid uptake, lipid synthesis, and/or modulation of ATGL action were not affected by genotype. Thus, in striking contrast to adipocyte-specific overexpression of ATGL (23), increasing IMTG hydrolysis via ATGL overexpression has minimal to no effect on other lipid metabolic pathways or mitochondrial phenotypes.

Increasing IMTG hydrolysis via ATGL overexpression does not influence systemic energy homeostasis, glucose homeostasis, or insulin action. Again, the expected effects of HFD feeding were noted. However, there were no effects of genotype on body weight (Fig. 7*A*), fat mass (Fig. 7*B*), lean mass (Fig. 7*C*), individual muscle weights (Fig. 7*D*), nonmuscle tissue weights (data not shown), total energy intake and energy expenditure (data not shown), or respiratory exchange ratio (RER) during fed-fasted-refed conditions (metabolic flexibility) (Fig. 7*E*). In addition, no differences in serum glucose were identified between genotypes following a physiological (4-h) fast (Fig. 7*G*, time 0 of ITT), a prolonged (12-h) fast (Fig. 7*F*, time 0 of GTT), an intraperitoneal glucose challenge (Fig. 7*F*, GTT), or an intraperitoneal insulin challenge (Fig. 7*G*, ITT). Consistent with these findings, diet but not genotype effects were identified in skeletal muscle–specific insulin-stimulated phosphorylation of key proteins in the insulin signaling cascade including insulin receptor substrate 1 (data not shown) and Akt (Akt pS^{473} or Akt pT^{308}) (Fig. 7*H–K*). Thus, increasing IMTG hydrolysis via ATGL overexpression does not influence systemic energy homeostasis or either systemic or muscle-specific glucose homeostasis and insulin action.

DISCUSSION

The goal of the current study was to determine the role of IMTGs and IMTG hydrolysis in skeletal muscle and whole-body metabolism at baseline and in response to diet-induced obesity. Remarkably, we demonstrate that modulation of IMTG content and hydrolysis by altering ATGL action in skeletal muscle does not influence systemic energy, lipid, or glucose homeostasis, nor does it influence muscle-specific insulin action or mitochondrial function. The absence of profound metabolic phenotypes in skeletal muscle–specific ATGL mutant mice is striking considering the dramatic changes in IMTG hydrolysis and accumulation. These data provide compelling evidence that IMTG content, while often highly associated with insulin resistance and metabolic disease, is not causal in these disorders. These data further indicate that modulating IMTG hydrolysis neither promotes nor protects against deleterious metabolic consequences of obesity.

Although the effects of skeletal muscle lipid uptake and oxidation on glucose homeostasis and insulin action have been extensively studied (11), the metabolic consequences of IMTG metabolism itself remain less well-understood (6). With regards to IMTG synthesis, increasing muscle DGAT1 in vivo promotes insulin sensitivity (13,14), whereas increasing DGAT2 promotes insulin resistance (15). While both interventions similarly increase IMTG content, they differentially affect other non-TAG lipid metabolites (ceramides), suggesting that the latter rather than the former influences metabolic phenotypes. Thus, different proteins may have different metabolic effects, despite affecting similar metabolic pathways. With regards to IMTG hydrolysis, acutely modulating ATGL or HSL action in cultured human myotubes alters DAGs and disrupts glucose homeostasis and insulin action (33). However, the current study indicates that chronically modulating ATGL action in murine skeletal muscle in vivo fails to influence metabolic phenotypes. Several potential adaptations (i.e., increased CGI-58, Plin2, and Plin5 in SMAKO mice) may protect against lipid-induced insulin resistance but are clearly not sufficient to fully compensate for altered IMTG hydrolysis. These data indicate that changing IMTG content by altering IMTG hydrolysis is not pathogenic. The validity of these conclusions is supported by the finding that comparable changes in IMTG content by altering IMTG synthesis are sufficient to influence metabolic outcomes (13–15), whereas changes in IMTG hydrolysis are not.

Interestingly, enhancing IMTG hydrolysis in vivo has minimal effect on non-TAG lipid metabolites, and inhibiting

control (*left*) and Tg (*right*) mice including general morphology by H&E staining (*top*) and IMTG content by ORO staining (*bottom*) (Line 1, ♂, 12 weeks, HFD for 4 weeks, fasted 12 h, GPS complex). *H*: IMTG content by ORO staining using quantitative IF (Line 1, ♂, 28 weeks, chow and HFD, fasted 12 h, GPS complex, average of four muscle areas each; *n* = 4/group). Type 2B fibers of chow-fed WT mice are arbitrarily set to 1. *I*: Intramyocellular DAG, ceramide, and FA-CoA content using biochemical analysis of whole muscle (Line 1, ♂, 28 weeks, chow and HFD, fasted 12 h, quadriceps; *n* = 3/group). For overall effects having $P < 0.05$: D, diet; F, fiber type; G, genotype; T, treatment (with HSL-inhibitor). For specific comparisons having $P < 0.05$: #for effect of diet; *for effect of genotype; and @for effect of treatment. AU, arbitrary units; BAT, brown adipose tissue; EDL, extensor digitorum longus; Gas, gastrocnemius; Hrt, heart; Panc, pancreas; PGAT, perigonadal adipose tissue; Quad, quadriceps; Sol, soleus; TA, tibialis anterior.

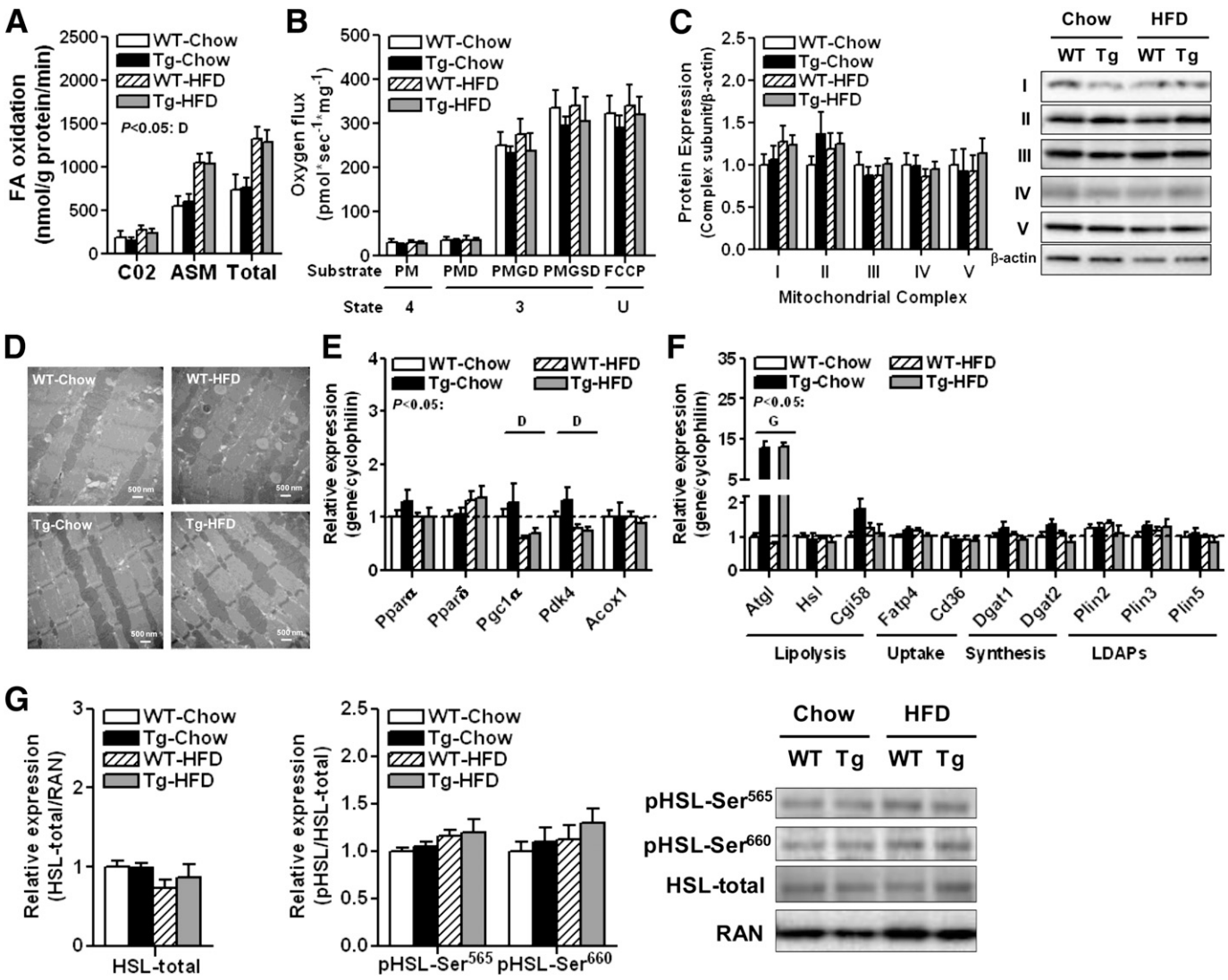

FIG. 6. Skeletal muscle mitochondrial function and expression of genes/proteins regulating lipid homeostasis in Ckm-ATGL mice. *A*: FA oxidation (♂, 28 weeks, fasted 12 h, red gastrocnemius; *n* = 5–8/group). *B*: Mitochondrial respiration in permeabilized muscle fibers (♂, 34 weeks, fasted 12 h, extensor digitorum longus; *n* = 3–6/group). *C*: Expression of oxidative phosphorylation proteins in complexes I–V (♂, 34 weeks, fasted 12 h, tibialis anterior; *n* = 4–7/group). Data are normalized to protein expression of β-actin. *D*: TEM of skeletal muscle (♂, 34 weeks, fasted 12 h, red quadriceps, representative images). mRNA expression of PPARα/PGC1α and their target genes (*E*) and genes for lipid breakdown (lipolysis), uptake, and synthesis as well as lipid droplet–associated proteins (LDAPs) of the Plin family (*F*) relative to cyclophilin control with expression in WT-chow normalized to 1 (♂, 34 weeks, tibialis anterior; *n* = 7–21/group). *G*: Protein expression of total HSL normalized to Ran GTPase (RAN) control (*left*), phosphorylated HSL normalized to total HSL (*middle*), and representative immunoblots (*right*) (♂, 34 weeks, tibialis anterior; *n* = 5–7/group). For mRNA and protein expression, samples were confirmed to have low or no expression of Plin1, thereby confirming absence of significant fat contamination. For overall effects having $P < 0.05$: D, diet; G, genotype.

IMTG hydrolysis increases certain subspecies of DAGs and tends to increase rather than decrease total DAGs. The lack of DAG accumulation with ATGL overexpression is likely due to sufficient residual capacity to further metabolize DAGs relative to the amount produced by IMTG hydrolysis. Furthermore, recent evidence suggests that the specific DAG species generated by ATGL cannot be directly used for phospholipid synthesis or activation of protein kinase C, mechanisms by which DAGs have been shown to influence glucose homoeostasis and insulin action (34). The reason why DAGs accumulate with ATGL deletion is less clear but also occurs in mice with global deletion of ATGL (17) and knockdown of the ATGL coactivator CGI-58 (35). Studies of the latter suggest that the increase in DAGs may result from compensatory increases in DAG synthesis without concomitant increases in TAG synthesis (35) and further suggests that the lack of a physiological effect likely results from their subcellular localization to lipid droplets rather than membranes (35). Besides subcellular localization, the type of DAG stereoisomer (i.e., sn-1–2 vs. sn-1–3 vs. sni-2–3) and FA composition may also contribute to the dissociation between DAG concentrations and insulin responsiveness (5). Hence, modulating IMTG hydrolysis in vivo may not influence glucose homeostasis and insulin responsiveness because it does not produce physiologically relevant changes in the amount or cellular localization of specific bioactive non-TAG lipid metabolites.

In contrast, altering TAG hydrolysis could also affect metabolic phenotypes by influencing mitochondrial function via activation of PPAR nuclear transcription factors. A role for ATGL-mediated TAG hydrolysis in ligand-dependent (36) and ligand-independent (37,38) PPARα activation has been demonstrated in nonskeletal muscle

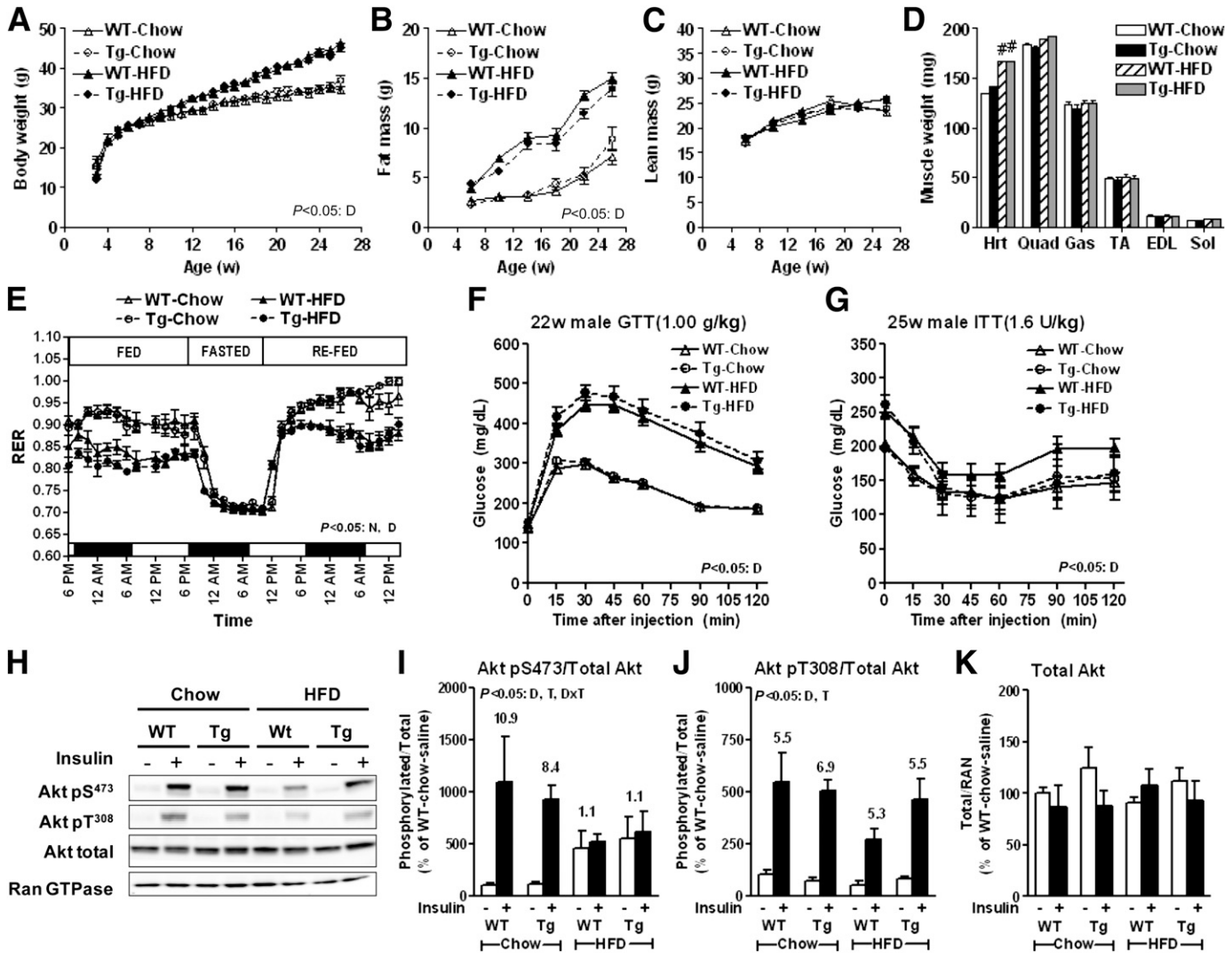

FIG. 7. Energy/glucose homeostasis and insulin action in Ckm-ATGL mice. Body weight (*A*), fat mass (*B*), and lean mass (*C*) (Line 1, ♂, 3–26 weeks; $n \geq 12$/group). *D*: Muscle weights (nonmuscle tissue weights also showed no genotype effects; data not shown). With the exception of heart, data represent the average weight for both muscles from each mouse (Line 1, ♂, 28 weeks, fasted 12 h; $n \geq 24$/group). EDL, extensor digitorum longus; Gas, gastrocnemius; Hrt, heart; Quad, quadriceps; Sol, soleus; TA, tibialis anterior. *E*: RER using a Comprehensive Lab Animal Monitoring System (CLAMS) (Line 1, ♂, 9 weeks, weight-matched; $n = 4$/group). *F*: GTT at 22 weeks with 1.0 g/kg glucose i.p. (♂, fasted 12 h; $n = 7$–22/group). *G*: ITT at 25 weeks with 1.6 units/kg insulin i.p. (Line 1, ♂, fasted 4 h; $n = 7$–22/group). *H–K*: Insulin signaling studies: Mice were fasted for 12 h, injected i.p. with saline or insulin at 10 units/kg body weight, and killed 10 min thereafter (♂, 34 weeks, tibialis anterior; $n = 5$–7/group). Representative immunoblots (*H*) and associated quantification of stoichiometric phosphorylation of Akt pS^{473}/Akt total (*I*), Akt pT^{308}/Akt total (*J*), and total Akt/Ran GTPase control (*K*). Fold change in response to insulin treatment is indicated above the black bars. For overall effects having $P < 0.05$: D, diet; N, nutritional status (i.e., fasting/refeeding); T, treatment (i.e., with insulin). For clarity, only overall effects are shown. For simple effects in *D*, #$P < 0.05$ for effect of diet.

cells. The physiological relevance of these findings has been corroborated in vivo in adipose tissue (23,39) and cardiac muscle (21). More recently, it has been shown that indirect modulation of ATGL action via its coactivator CGI-58 in human myotubes (40) or via Plin5 in rat muscle (41) influences PPAR target genes and mitochondrial function. Unexpectedly, changes in ATGL-mediated TAG hydrolysis in skeletal muscle in vivo do not significantly impact these parameters. These results are consistent with reports demonstrating IMTG accumulation but unaltered in vivo mitochondrial function in skeletal muscle of GAKO (42) and muscle-specific CGI-58 knockout mice (43). Thus, in striking contrast to cardiac muscle (21), in vivo modulation of TAG hydrolysis in skeletal muscle does not influence PPAR target genes or mitochondrial phenotypes.

The divergent consequences of altering IMTG hydrolysis in cardiac versus skeletal muscle may be due to differences in metabolic flux (10,44). In cardiac muscle (variable energy supply, chronically high energy demand), it has been proposed that FAs are preferentially directed to IMTG storage followed by coordinated ATGL-mediated release as energy substrates and PPAR ligands, thereby coupling hydrolysis to oxidation (21). In skeletal muscle (variable energy supply and demand), the above processes may only become physiologically relevant during functional but not nutritional stresses. Interestingly, enhancing TAG synthesis (via DGAT1) in rodent skeletal muscle (14,45) or TAG hydrolysis (via ATGL) in rodent adipose tissue are sufficient to drive FA oxidation (23) in the absence of functional stress, whereas enhancing TAG hydrolysis (via ATGL) in rodent skeletal muscle is not. While prior studies have suggested that ATGL-mediated TAG hydrolysis is important for working muscle (19,46), these studies were performed using GAKO mice, which have

significant cardiac morbidity and defects in TAG catabolism in multiple tissues. Therefore, additional studies are required to determine the relative contribution of extra- versus intramyocellular TAG hydrolysis to skeletal muscle metabolism/function during functional stresses such as endurance or resistance exercise, which are believed to increase flux through the IMTG pool.

The regulated storage and release of both essential and deleterious lipid metabolites from intracellular TAG stores are among the most fundamental processes in metabolism. The complex relationship between intracellular TAGs and metabolic phenotypes is best exemplified in skeletal muscle, where IMTG accumulation is variably associated with insulin resistance (i.e., obesity) or insulin sensitivity (i.e., endurance exercise). The resolution of how IMTG metabolism contributes to these divergent phenotypes holds the key to understanding how these processes may be exploited for therapeutic benefit. Our study provides convincing evidence that IMTGs neither cause nor prevent insulin resistance and that manipulation of IMTG hydrolysis via altered ATGL action does not influence metabolic consequences of HFD-induced obesity. Additional functional studies will further enhance our understanding of TAG hydrolysis in muscle and whole-body physiology. Importantly, with few exceptions (21,47), tissue-specific modulation of ATGL-mediated TAG hydrolysis has largely produced beneficial effects (23,39,48–50). Thus, the lack of adverse metabolic consequences of altering ATGL action in skeletal muscle indicates that modulating TA hydrolysis may still be a viable therapeutic strategy for treating metabolic disorders. Additional studies in other metabolically relevant tissues are still required to more fully understand the health implications of TAG hydrolysis in normal physiology and disease.

ACKNOWLEDGMENTS

This work was supported by the following: National Institutes of Health grants R03-DK-077697 and R01-DK-090166 and a Howard Hughes Medical Institute Physician-Scientist Early Career Award (to E.E.K.); Claude D. Pepper Pilot Grant (to M.T.S.); Erwin Schrödinger Fellowship (to G.S.); and the Endocrine Fellows Foundation's Marilyn Fishman Grant for Diabetes Research (to C.F.Y.). Tissue lipid analysis was supported in part by the Lipidomics Shared Resource, Hollings Cancer Center, Medical University of South Carolina (P30-CA-138313); the Lipidomics Core in the SC Lipidomics and Pathobiology COBRE (P20-RR-017677); the National Center for Research Resources; and the Office of the Director of the National Institutes of Health (C06-RR-018823).

No potential conflicts of interest relevant to this article were reported.

M.T.S. and M.K.B. were project leaders for analysis of SMAKO and Ckm-ATGL mice, respectively. L.C. was the technical manager for all experiments and performed imaging analyses. G.S. and C.F.Y. performed experiments. G.D., B.H.G., and P.C. assessed mitochondrial respiration. V.R. and J.P.D. quantified FA-CoAs. R.S. and R.Z. performed TAG hydrolase activities. D.B.S. performed imaging analysis. N.P.G. helped generate and validate the mouse models. P.C.K. and T.P. contributed intellectual expertise and helped prepare the manuscript. E.E.K. generated mouse models, designed, executed, and analyzed experiments, and wrote the manuscript. All authors contributed intellectually to this work and reviewed and edited the manuscript. E.E.K. is the guarantor of this work and, as such, had full access to all the data in the study and takes responsibility for the integrity of the data and the accuracy of the data analysis.

Parts of this study were presented in poster form at the 73rd Scientific Sessions of the American Diabetes Association, Chicago, Illinois, 21–25 June 2013.

The authors thank the following for contributions: Jeffrey S. Flier, MD (Harvard Medical School) for mentoring and support; Eric Olson, PhD (University of Texas Southwestern) for providing Myo-Cre mice; C. Ronald Kahn, MD (Joslin Diabetes Center) for providing the Ckm promoter construct; Jacek Bielawski, PhD (Medical University of South Carolina) for expertise related to lipidomics; the University of Pittsburgh Center for Biological Imaging for equipment and expertise related to imaging; and the University of Pittsburgh Division of Endocrinology Metabolic Center for equipment and expertise related to metabolism.

REFERENCES

1. Schaffer JE. Lipotoxicity: when tissues overeat. Curr Opin Lipidol 2003;14:281–287
2. Goodpaster BH, He J, Watkins S, Kelley DE. Skeletal muscle lipid content and insulin resistance: evidence for a paradox in endurance-trained athletes. J Clin Endocrinol Metab 2001;86:5755–5761
3. Samuel VT, Shulman GI. Mechanisms for insulin resistance: common threads and missing links. Cell 2012;148:852–871
4. Cowart LA. Sphingolipids: players in the pathology of metabolic disease. Trends Endocrinol Metab 2009;20:34–42
5. Amati F. Revisiting the diacylglycerol-induced insulin resistance hypothesis. Obes Rev 2012;13(Suppl. 2):40–50
6. Bosma M, Kersten S, Hesselink MK, Schrauwen P. Re-evaluating lipotoxic triggers in skeletal muscle: relating intramyocellular lipid metabolism to insulin sensitivity. Prog Lipid Res 2012;51:36–49
7. Coen PM, Goodpaster BH. Role of intramyocelluar lipids in human health. Trends Endocrinol Metab 2012;23:391–398
8. van Loon LJ, Goodpaster BH. Increased intramuscular lipid storage in the insulin-resistant and endurance-trained state. Pflugers Arch 2006;451:606–616
9. Goodpaster BH. Mitochondrial deficiency is associated with insulin resistance. Diabetes 2013;62:1032–1035
10. Funai K, Semenkovich CF. Skeletal muscle lipid flux: running water carries no poison. Am J Physiol Endocrinol Metab 2011;301:E245–E251
11. Zhang L, Keung W, Samokhvalov V, Wang W, Lopaschuk GD. Role of fatty acid uptake and fatty acid beta-oxidation in mediating insulin resistance in heart and skeletal muscle. Biochim Biophys Acta 2010;1801:1–22
12. Holloszy JO. "Deficiency" of mitochondria in muscle does not cause insulin resistance. Diabetes 2013;62:1036–1040
13. Liu L, Zhang Y, Chen N, Shi X, Tsang B, Yu YH. Upregulation of myocellular DGAT1 augments triglyceride synthesis in skeletal muscle and protects against fat-induced insulin resistance. J Clin Invest 2007;117:1679–1689
14. Liu L, Shi X, Choi CS, et al. Paradoxical coupling of triglyceride synthesis and fatty acid oxidation in skeletal muscle overexpressing DGAT1. Diabetes 2009;58:2516–2524
15. Levin MC, Monetti M, Watt MJ, et al. Increased lipid accumulation and insulin resistance in transgenic mice expressing DGAT2 in glycolytic (type II) muscle. Am J Physiol Endocrinol Metab 2007;293:E1772–E1781
16. Haemmerle G, Lass A, Zimmermann R, et al. Defective lipolysis and altered energy metabolism in mice lacking adipose triglyceride lipase. Science 2006;312:734–737
17. Kienesberger PC, Lee D, Pulinilkunnil T, et al. Adipose triglyceride lipase deficiency causes tissue-specific changes in insulin signaling. J Biol Chem 2009;284:30218–30229
18. Hoy AJ, Bruce CR, Turpin SM, Morris AJ, Febbraio MA, Watt MJ. Adipose triglyceride lipase-null mice are resistant to high-fat diet-induced insulin resistance despite reduced energy expenditure and ectopic lipid accumulation. Endocrinology 2011;152:48–58
19. Huijsman E, van de Par C, Economou C, et al. Adipose triacylglycerol lipase deletion alters whole body energy metabolism and impairs exercise performance in mice. Am J Physiol Endocrinol Metab 2009;297:E505–E513
20. Kraemer FB, Shen WJ. Hormone-sensitive lipase knockouts. Nutr Metab (Lond) 2006;3:12

21. Haemmerle G, Moustafa T, Woelkart G, et al. ATGL-mediated fat catabolism regulates cardiac mitochondrial function via PPAR-α and PGC-1. Nat Med 2011;17:1076–1085
22. Reid BN, Ables GP, Otlivanchik OA, et al. Hepatic overexpression of hormone-sensitive lipase and adipose triglyceride lipase promotes fatty acid oxidation, stimulates direct release of free fatty acids, and ameliorates steatosis. J Biol Chem 2008;283:13087–13099
23. Ahmadian M, Duncan RE, Varady KA, et al. Adipose overexpression of desnutrin promotes fatty acid use and attenuates diet-induced obesity. Diabetes 2009;58:855–866
24. Li S, Czubryt MP, McAnally J, et al. Requirement for serum response factor for skeletal muscle growth and maturation revealed by tissue-specific gene deletion in mice. Proc Natl Acad Sci USA 2005;102:1082–1087
25. Brüning JC, Michael MD, Winnay JN, et al. A muscle-specific insulin receptor knockout exhibits features of the metabolic syndrome of NIDDM without altering glucose tolerance. Mol Cell 1998;2:559–569
26. Basantani MK, Sitnick MT, Cai L, et al. Pnpla3/Adiponutrin deficiency in mice does not contribute to fatty liver disease or metabolic syndrome. J Lipid Res 2011;52:318–329
27. Bielawski J, Szulc ZM, Hannun YA, Bielawska A. Simultaneous quantitative analysis of bioactive sphingolipids by high-performance liquid chromatography-tandem mass spectrometry. Methods 2006;39:82–91
28. Sun D, Cree MG, Wolfe RR. Quantification of the concentration and ^{13}C tracer enrichment of long-chain fatty acyl-coenzyme A in muscle by liquid chromatography/mass spectrometry. Anal Biochem 2006;349:87–95
29. Berggren JR, Boyle KE, Chapman WH, Houmard JA. Skeletal muscle lipid oxidation and obesity: influence of weight loss and exercise. Am J Physiol Endocrinol Metab 2008;294:E726–E732
30. Kuznetsov AV, Veksler V, Gellerich FN, Saks V, Margreiter R, Kunz WS. Analysis of mitochondrial function in situ in permeabilized muscle fibers, tissues and cells. Nat Protoc 2008;3:965–976
31. Koopman R, Schaart G, Hesselink MK. Optimisation of oil red O staining permits combination with immunofluorescence and automated quantification of lipids. Histochem Cell Biol 2001;116:63–68
32. Kershaw EE, Hamm JK, Verhagen LA, Peroni O, Katic M, Flier JS. Adipose triglyceride lipase: function, regulation by insulin, and comparison with adiponutrin. Diabetes 2006;55:148–157
33. Badin PM, Louche K, Mairal A, et al. Altered skeletal muscle lipase expression and activity contribute to insulin resistance in humans. Diabetes 2011;60:1734–1742
34. Eichmann TO, Kumari M, Haas JT, et al. Studies on the substrate and stereo/regioselectivity of adipose triglyceride lipase, hormone-sensitive lipase, and diacylglycerol-O-acyltransferases. J Biol Chem 2012;287:41446–41457
35. Cantley JL, Yoshimura T, Camporez JP, et al. CGI-58 knockdown sequesters diacylglycerols in lipid droplets/ER-preventing diacylglycerol-mediated hepatic insulin resistance. Proc Natl Acad Sci USA 2013;110:1869–1874
36. Mottillo EP, Bloch AE, Leff T, Granneman JG. Lipolytic products activate peroxisome proliferator-activated receptor (PPAR) α and δ in brown adipocytes to match fatty acid oxidation with supply. J Biol Chem 2012;287:25038–25048
37. Ong KT, Mashek MT, Bu SY, Greenberg AS, Mashek DG. Adipose triglyceride lipase is a major hepatic lipase that regulates triacylglycerol turnover and fatty acid signaling and partitioning. Hepatology 2011;53:116–126
38. Sapiro JM, Mashek MT, Greenberg AS, Mashek DG. Hepatic triacylglycerol hydrolysis regulates peroxisome proliferator-activated receptor alpha activity. J Lipid Res 2009;50:1621–1629
39. Ahmadian M, Abbott MJ, Tang T, et al. Desnutrin/ATGL is regulated by AMPK and is required for a brown adipose phenotype. Cell Metab 2011;13:739–748
40. Bosma M, Sparks LM, Hooiveld GJ, et al. Overexpression of PLIN5 in skeletal muscle promotes oxidative gene expression and intramyocellular lipid content without compromising insulin sensitivity. Biochim Biophys Acta 2013;1831:844–852
41. Badin PM, Loubière C, Coonen M, et al. Regulation of skeletal muscle lipolysis and oxidative metabolism by the co-lipase CGI-58. J Lipid Res 2012;53:839–848
42. Nunes PM, van de Weijer T, Veltien A, et al. Increased intramyocellular lipids but unaltered in vivo mitochondrial oxidative phosphorylation in skeletal muscle of adipose triglyceride lipase-deficient mice. Am J Physiol Endocrinol Metab 2012;303:E71–E81
43. Zierler KA, Jaeger D, Pollak NM, et al. Functional cardiac lipolysis in mice critically depends on comparative gene identification-58. J Biol Chem 2013;288:9892–9904
44. Muoio DM, Koves TR. Skeletal muscle adaptation to fatty acid depends on coordinated actions of the PPARs and PGC1 alpha: implications for metabolic disease. Appl Physiol Nutr Metab 2007;32:874–883
45. Timmers S, de Vogel-van den Bosch J, Hesselink MK, et al. Paradoxical increase in TAG and DAG content parallel the insulin sensitizing effect of unilateral DGAT1 overexpression in rat skeletal muscle. PLoS ONE 2011;6:e14503
46. Schoiswohl G, Schweiger M, Schreiber R, et al. Adipose triglyceride lipase plays a key role in the supply of the working muscle with fatty acids. J Lipid Res 2010;51:490–499
47. Wu JW, Wang SP, Alvarez F, et al. Deficiency of liver adipose triglyceride lipase in mice causes progressive hepatic steatosis. Hepatology 2011;54:122–132
48. Das SK, Eder S, Schauer S, et al. Adipose triglyceride lipase contributes to cancer-associated cachexia. Science 2011;333:233–238
49. Kienesberger PC, Pulinilkunnil T, Sung MM, et al. Myocardial ATGL overexpression decreases the reliance on fatty acid oxidation and protects against pressure overload-induced cardiac dysfunction. Mol Cell Biol 2012;32:740–750
50. Pulinilkunnil T, Kienesberger PC, Nagendran J, et al. Myocardial adipose triglyceride lipase overexpression protects diabetic mice from the development of lipotoxic cardiomyopathy. Diabetes 2013;62:1464–1477